

# The Stellar Content of Obscured Galactic Giant<sup>1</sup> H II Regions: I. W43

R. D. Blum<sup>2</sup>

Cerro Tololo Interamerican Observatory, Casilla 603, La Serena, Chile  
rblum@noao.edu

A. Damineli<sup>2,3</sup>

IAG-USP, Av. Miguel Stefano 4200, 04301-904, Sao Paulo, Brazil  
daminieli@iagusp.usp.br

P. S. Conti

JILA, University of Colorado  
Campus Box 440, Boulder, CO, 80309  
pconti@casa.colorado.edu

*accepted for publication in the Astronomical Journal*

## ABSTRACT

Near infrared images of the Galactic giant H II region W43 reveal a dense stellar cluster at its center. Broad band *JHK* photometry of the young cluster and *K*-band spectra of three of its bright stars are presented. The 2  $\mu\text{m}$  spectrum of the brightest star in the cluster is very well matched to the spectra of Wolf-Rayet stars of sub-type WN7. Two other stars are identified as O type giants or supergiants by their N III and C IV emission. The close spatial clustering of O and the hydrogen WN type stars is analogous to the intense star burst clusters R136 in the Large Magellanic Cloud and NGC 3603 in the Galaxy.

*Subject headings:* H II regions — infrared: stars — stars: early-type — stars: fundamental parameters

---

<sup>1</sup> In this series of papers we shall follow a suggestion of Dr. Robert Kennicutt (private communication) that “giant” means that more than  $10^{50}$  Lyman continuum photons are inferred to be emitted per second from the H II region. This is about ten times the luminosity of the Orion nebula and roughly the number emitted from the hottest *single* O3-type star. As these stars are not found in isolation, there is an implication that a “giant” H II region contains some minimum of *multiple* O-type stars.

<sup>2</sup>Visiting Astronomer, Cerro Tololo Interamerican Observatory, National Optical Astronomy Observatories, which is operated by Associated Universities for Research in Astronomy, Inc., under cooperative agreement with the National Science Foundation

## 1. INTRODUCTION

Near infrared (1–5  $\mu\text{m}$ ) spectroscopic classification schemes have recently been outlined for OB stars (Hanson et al. 1996, hereafter HCR96; Blum et al. 1997) and Wolf–Rayet (WR) stars (e.g., Eenens et al. 1991; Figer et al. 1997). Coupled with infrared spectrometers on large telescopes, these classification schemes are now pushing forward the exploration of optically obscured, young stellar populations throughout the inner Galaxy. Indeed, Hanson et al. (1997) have presented a detailed investigation of the ionizing O and B stars in M17, a relatively nearby but partially obscured giant HII region. In addition, the central 50 pc of the Milky Way have been intensely studied with the application of near infrared spectroscopy. It has been revealed that the stellar cluster in the central parsec, as well as two other nearby clusters, are rich in OB and Wolf–Rayet stars (see Morris & Serabyn 1996 for a recent review and the many references therein).

Massey et al. (1995) have produced a detailed characterization of the stellar mass function in optically visible OB associations in the Milky Way. Their fundamental work serves as a benchmark comparison of Galactic OB star properties relative to other environments (e.g., the Magellanic Clouds). The present project, in which this paper is a beginning, will build on Massey et al.’s work by investigating the optically obscured stellar content of the inner Galaxy giant H II regions through infrared photometry and spectroscopy. These observations will probe and compare the mass function as a function of Galacto–centric position, provide checks on Galactic structure (spiral arm morphology) through spectroscopic distance estimates which can be compared to radio recombination line/rotation model distances, and investigate massive star formation phenomena. The latter aspect is particularly exciting as many of the optically obscured giant H II regions are young enough that we expect to find multiple epochs of star formation, i.e., young stellar objects (YSOs) in the presence of more evolved OB and WR stars. This is already in evidence in M 17 where it appears that while the hottest O stars have little or no infrared excess (having “blown” away their birth cocoons), the somewhat less massive later type O and B stars show evidence for discs still surrounding them (Hanson et al. 1997). These two groups are spatially segregated in M 17. Are the early O stars more efficient at removing their circumstellar material through strong winds and radiation, or do the two groups represent star formation at different epochs in M 17? Investigations of other giant H II regions will help answer such fundamental questions about massive star formation.

W43 (=G30.8-0.2) is a giant H II region in the first Galactic quadrant ( $l, b = 30.8, -0.2$ ). Its distance, from H I line radio measurements and a Galactic rotation model, is about 7 kpc (Smith et al. 1978). The entire region emits about  $10^{51}$  Lyman continuum photons per sec (= Lyc) according to these authors. This is equivalent to roughly 100 “O7 star equivalents”

(Vacca 1994), similar to NGC 3603 and a factor of a few smaller than R136. W43 contains about  $10^6$  solar masses of molecular gas, a quantity which suggests ongoing star formation (Liszt 1995). W43 has been observed by Liszt et al. (1993) with the Very Large Array (VLA): they provide a  $9' \times 9'$  scale map in the radio L band continuum synthesized from the H I absorption measures. The overall spatial morphology of the emission is roughly that of a “T” with a sagging “wing” to the west. Subrahmanyan & Goss (1996) present an  $80' \times 80'$  VLA map of the entire W43 complex at 330 MHz; a number of other sources are indicated, but G30.8-0.2 dominates the radio emission. Liszt et al. (1993) call the position of the strongest source G30.78–0.23; this is the top bar of the “T”. This source is called G30.8N in the far infrared maps of Lester et al. (1985). The bottom of the “T”, also seen in the far infrared maps, is denoted G30.8S by Lester et al. (1985). The stellar cluster, which will be the main topic of this paper, lies between G30.8N and G30.8S and was first seen as an unresolved  $K$ –band source by Lester et al. (1985).

Using  $J$ ,  $H$ , and  $K$ –band photometry, we reveal this stellar source as a massive cluster of newly formed stars. Three of the most luminous stars in the cluster are identified and classified as hot stars. W43 is totally obscured optically; we estimate (below) that  $A_V$  is about 30 mag.

## 2. OBSERVATIONS AND DATA REDUCTION

High angular resolution  $J$ ,  $H$ , and  $K$  images of W43 were obtained on the nights of 28 and 29 August 1998 with the f/14 tip-tilt system on the Cerro Tololo Interamerican Observatory (CTIO) 4m Blanco telescope using the facility imager (CIRIM). The spectroscopic data were obtained on the night of 02 June 1998 using the f/14 tip-tilt system at the Blanco telescope with the facility infrared spectrometer (IRS). Spectroscopic pointings were made from preliminary images taken with the Cryogenic Optical Bench (COB) obtained on 24 April 1997. CIRIM is described in the instrument manual found on the CTIO www pages (www.ctio.noao.edu). The tip-tilt system, COB imager, and IRS are described on the CTIO www pages as well as by Pérez & Elston (1998), Probst et al. (1994), and DePoy et al. (1990), respectively. Briefly, the tip-tilt system uses three piezo-electric actuators to move the secondary mirror at high frequency in a computer controlled feed-back loop to compensate for image centroid motion. COB employs  $0.094''$  pixels, the IRS  $0.32''$  pixels, and CIRIM  $0.21''$  pixels.

All basic data reduction was accomplished using IRAF<sup>3</sup>. Each image/spectrum was

---

<sup>3</sup>IRAF is distributed by the National Optical Astronomy Observatories.

flat-fielded using dome flats and then sky subtracted using a median combined image of five to six frames. For W43 itself, independent sky frames were obtained five arcminutes east and/or south of the cluster. Standard stars used the median combination of the data for sky.

## 2.1. Images

The CIRIM image data were obtained under photometric conditions and in  $0.50'' \lesssim \text{FWHM} \lesssim 0.80''$  seeing (this includes the tip-tilt correction). Total exposure times were 720 s, 90 s, and 90 s at  $J$ ,  $H$ , and  $K$ , respectively. The individual  $J$ ,  $H$ , and  $K$  frames were shifted and combined. DAOPHOT (Stetson 1987) photometry was performed on the combined images using brighter stars off the cluster center for the psf reference (The LickVista 5.0 version of DAOPHOT was used). The flux calibration was accomplished using standards 9172 and 9178 from Persson et al. (1998) which are essentially on the CIT/CTIO photometric system (see the discussion on color transformations in Persson et al. 1998). The standards were taken just before and after the W43 data, bracketing the airmass of W43, except for the  $K$ -band images for which the standard and W43 were within 0.1 airmass of each other. Aperture corrections using 8 pixel radius apertures were used to put the instrumental magnitudes on the CTIO/CIT system. The central star in the cluster was saturated in the CIRIM  $K$ -band images. Its magnitude has been corrected (by 0.06 mag) using the preliminary COB data taken in 1997. The  $J$ -band data include a color correction as given in the CIRIM manual ( $-0.037 \times J - K$ ).

Uncertainties for the final  $JHK$  magnitudes include the formal DAOPHOT error added in quadrature to the error in the mean of the photometric standards. The latter was derived from the scatter in the individual measurements and was  $\pm 0.027$ ,  $\pm 0.022$ ,  $\pm 0.013$  mag in  $J$ ,  $H$ , and  $K$ , respectively. The DAOPHOT errors ranged from approximately  $\pm 0.01$  mag to an arbitrary cut-off of 0.5 mag (stars with larger errors were excluded from further analysis).

Lower angular resolution images were obtained at  $J$ ,  $H$ , and  $K$  using CIRIM at f/13.5 on the CTIO 1.5m ( $0.65'' \text{ pix}^{-1}$ ). The individual  $J$ ,  $H$ , and  $K$  frames were shifted and combined and have measured seeing of  $\approx 1.5''$  FWHM. While these low resolution images are calibrated, their photometry is not discussed further in this paper. They are used only to discuss the morphology of the region surrounding the high resolution images of the W43 cluster.

## 2.2. Spectra

The spectra were obtained with a  $0.65''$  wide slit (oriented NS) in  $\lesssim 1''$  seeing and divided by the spectrum of HD7209 (A1V) to remove telluric absorption features.  $\text{Br}\gamma$  absorption in HD7209 was removed by eye by drawing a line across it between two continuum points. One dimensional spectra were obtained by extracting and summing the flux in a  $\pm 2$  pixel aperture.

The wavelength calibration was accomplished by measuring the positions of six bright  $\text{OH}^-$  lines from the  $K$ -band sky spectrum (Oliva & Origlia 1992). Because the grating was moved when acquiring objects, the zero point of the solution is good only to a few pixels; lines are identified by their relative difference between one and another. The measured dispersion is  $0.001323 \mu\text{m pix}^{-1}$ . The spectral resolution at  $2.2 \mu\text{m}$  is  $\lambda/\Delta\lambda \approx 800$ .

## 3. RESULTS

### 3.1. Images

$J$ ,  $H$ , and  $K$  high angular resolution images are shown in Figure 1. The presence of a highly reddened cluster is immediately apparent. An unresolved  $K$ -band source was reported at this position by Lester et al. (1985). The source was not centered on the far infrared peaks in their maps, but was centered on a peak in a 6 cm radio map which they also presented. We discuss the position of the cluster relative to the far infrared emission and radio sources in §3.1.2. Cotera & Simpson (1997) also noted the presence of a stellar cluster from narrow-band images at  $2 \mu\text{m}$  (see §3.2), probably at this location.

#### 3.1.1. Color-Magnitude and Color-Color Plots

The  $K$  vs.  $H - K$  color-magnitude diagram (CMD) is given in Figure 2. This diagram is derived from a roughly  $58'' \times 58''$  area around the central cluster. The CMD shows a cluster sequence near  $H - K$   $1.8 \pm 0.4$  mag. The observed scatter is attributed to differential reddening (see below). Stars W43 #1, W43 #2, and W43 #3, for which spectra are presented, are labeled on the diagram. The main sequence is also shown in Figure 2 for O3 to B9 stars (Vacca et al. 1996, O3–B0 ; Schmidt-Kaler 1982, B1–B9) assuming a distance of 7 kpc (§1).

Figure 3 shows a  $J - H$  vs.  $H - K$  color-color plot of the stars on the high resolution

CIRIM images. This diagram indicates a large range in extinction and reddening in the field ( $0 \lesssim A_K \lesssim 4.5$  mag for stars detected at  $J$ ,  $H$ , and  $K$ ). The *dashed* lines in this plot represent reddening lines due to interstellar extinction based on the average relation given in Mathis (1990). Each of the two lines begins at the colors for an unreddened star (M3 III, Frogel et al. 1978; O6, Koornneef 1983). The lines describe an envelope of reddened colors for a nearby “disk” population with the above mean colors. From Figure 2, it is clear that the cluster sequence lies near  $H - K \sim 2$  mag. This corresponds to  $A_K$  of roughly 3.2 mag (or  $A_V \approx 34$  mag). Estimates of the  $A_K$  toward the spectroscopic targets are made in §3.2 where the spectroscopic clarification is used to determine the intrinsic colors of the stars.

Several objects on the color–color plot have a large excess emission indicated. Such excesses are consistent with the objects being YSOs with circumstellar material (e.g., a disk as indicated for a number of newly formed stars in M 17 – Hanson et al. 1997, though we have no evidence yet for any particular geometry giving rise to the putative excess emission in this case). There are also objects which appear extremely red in Figure 2 but which are not detected in  $J$ . These may be seen through even larger columns of obscuring material. Alternately, they may be intrinsically fainter at  $J$  but have a larger excess at  $K$ . These possibilities will be investigated with future spectroscopic observations.

### 3.1.2. Wide Field of View Image

A  $JHK$  color composite of the wide field of view CIRIM images ( $2.7' \times 2.7'$ ) is shown in Figure 4. This composite demonstrates that much of the scatter in Figure 2 (especially in the cluster sequence) can be attributed to differential reddening. The spatial scales involved can be quite small. For example, there is an obvious clump of obscuring material which appears in projection just arcseconds to the SW of the central cluster.

Along the upper edge of Figure 4 nebulosity (from  $\text{Br}\gamma$ ) is present. This is the upper part of the “T” so obvious in the radio and far infrared images (Lester et al. 1985; Liszt et al. 1993), and denoted by Lester et al. as G30.8N. Very red stars appear in projection against G30.8N in the color image. Notice that in the  $JHK$  color image there is *no* obvious vertical part of the “T”. However, there is nebulosity and (again) a clustering of red stars to the southeast of the cluster. This is part of the far infrared source which Lester et al. (1985) call G30.8S. According to Lester et al. (1985) there are two radio sources in between G30.8N and G30.8S which lie in a pronounced minimum of the far infrared emission. The western one of these was described by them as an unresolved  $K$ –band source ( $\sim 8$ th magnitude) which they claimed was the source of ionization for G30.8. This claim is confirmed in great detail by the images and spectra presented here. We have confirmed

the location of the Lester et al.  $K$ -band source as the stellar cluster by comparing our near infrared images to a Digitized Sky Survey <sup>4</sup> image centered on their coordinates ( $\alpha_{1950} = 18^{\text{h}} 45^{\text{m}} 00^{\text{s}}$ ,  $\delta_{1950} = -01^{\circ} 59' 54''$ ).

### 3.2. Spectra

The spectroscopic targets, W43 #1, #2, and #3 (Figures 5, 6, 7), were chosen from the preliminary COB CMD mentioned in §2.1 (similar but not as deep as Figure 2) as the brightest likely members of the central cluster. The second brightest star is only  $0.5''$  E of W43 #1 and was not observed spectroscopically because of its proximity to W43 #1. The effect of this star on the spectrum of W43 #1 should not be too great since it was placed outside the  $0.65''$  slit, has similar color to W43 #1, and is only 25% as bright as W43 #1.

#### 3.2.1. W43 #1

The line widths and equivalent widths (EW) of W43 #1 are given in Table 1 and compare well with those in Figer et al. (1997) for WR 131, a WN7 star of the hydrogen rich nitrogen sequence. The strong N III  $2.1155 \mu\text{m}$  He II  $2.189 \mu\text{m}$  and  $\text{Br}\gamma + \text{He I}$  (near  $2.17 \mu\text{m}$ ) emission are the signatures of a WN star. Cotera & Simpson (1997) report He II emission in narrow-band near infrared images of W43. This WN star is probably the source of the emission they observed. There is some similarity among the  $K$ -band spectra of some Of stars and late type WN stars (Conti et al. 1995), but the excellent match to the spectrum for WR131 for W43 #1 and the large line widths ( $\sim 1400 \text{ km s}^{-1}$ ) argue strongly for a WN classification. Comparing the line EW's and line widths to the other WN stars in Figer et al. (1997) indicates that W43 #1 is not as hot as a WN6 type because these objects show stronger He II ( $2.19 \mu\text{m}$ ) emission relative to  $\text{Br}\gamma$ . W43 #1 does not appear as cool as later type WN8 and WN9 stars which exhibit weaker He II emission and/or much stronger He I ( $2.06 \mu\text{m}$ ) emission. The long slit image of W43 #1 indicates no significant nebular contamination to the stellar spectrum. Comparison to the line ratios in Figer et al.

---

<sup>4</sup> Based on photographic data obtained using The UK Schmidt Telescope. The UK Schmidt Telescope was operated by the Royal Observatory Edinburgh, with funding from the UK Science and Engineering Research Council, until 1988 June, and thereafter by the Anglo-Australian Observatory. Original plate material is copyright (c) the Royal Observatory Edinburgh and the Anglo-Australian Observatory. The plates were processed into the present compressed digital form with their permission. The Digitized Sky Survey was produced at the Space Telescope Science Institute under US Government grant NAG W-2166.

(1997) also suggests this is the case.

As noted above, W43 #1 has a  $K$ -band spectrum similar to the optically classified WN7 star WR 131 (Figer et al. 1997). More precisely, WR 131 has an optical spectral classification of WN7+*abs*, where +*abs* refers to absorption lines seen in the *optical* spectrum. The absorption has some times been attributed to an unresolved companion star. While there is no evidence of absorption in the  $K$ -band spectrum of W43 #1 or the  $K$ -band spectrum of WR 131, it is possible that W43 #1 also has such a companion. This possibility is suggested by the fact that the standard star WN7  $K$ -band spectra appear to show a relative dilution of the  $K$ -band features between those stars with and without *optical* absorption lines (Figer et al. 1997, compare WR120 and WR131; also P. Eenens, private communication). And, it is the standards with the +*abs* to which W43 #1 is most similar.

### 3.2.2. W43 #2

The spectrum of W43 #2 is shown in Figure 6. N III at  $2.1155\ \mu\text{m}$ , is clearly detected. The N III emission suggests that W43 #2 is a mid to early O star (HCR96). In addition, there appears to be weak C IV emission at  $2.078\ \mu\text{m}$  (this line is typically less than one angstrom EW in somewhat higher resolution spectra of O stars, HCR) and perhaps some stellar Br $\gamma$  emission. The overall Br $\gamma$  feature is predominately nebular emission; it is difficult to perfectly remove this contribution as it is not uniform across the slit and this region of the spectrum was necessarily corrected with the telluric standard. He II  $2.189\ \mu\text{m}$  absorption is not detected but can be weak or in emission for supergiant O stars (HCR). The absence of He II  $2.189\ \mu\text{m}$  absorption in the spectrum of W43 #2 may be naturally explained if it is a supergiant. A supergiant classification is consistent with its position in the  $K$  v.  $H - K$  CMD (Figure 2; see below). The He I line at  $2.06\ \mu\text{m}$  is in absorption but this is probably an over-subtracted nebular contribution and/or imperfect telluric absorption correction.

### 3.2.3. W43 #3

W43 #3 has a  $K$ -band spectrum (Figure 7) which suggests it too is an O star. N III is detected as well as C IV emission. The  $2.078\ \mu\text{m}$  line appears slightly weak relative to the  $2.069\ \mu\text{m}$  line (the former is typically stronger; see HCR). This may not be too much of a concern in light of the weakness of the lines and the apparent signal to noise. Strong



emission features at He I  $2.06\ \mu\text{m}$  and  $\text{Br}\gamma$  are also present. He I  $2.06\ \mu\text{m}$  is not expected in normal O star spectra (HCR96) so this emission (and similarly  $\text{Br}\gamma$ ) is likely nebular. In addition, there is non-uniform nebular emission in the long slit image of W43 #3. Weak He II  $2.189\ \mu\text{m}$  absorption may be present in this spectrum ( $\text{EW} \lesssim 1.5\ \text{\AA}$ ) but the S/N in the region around  $2.189\ \mu\text{m}$  is insufficient for an accurate measurement (the feature to the red side of  $2.189\ \mu\text{m}$  is due to incomplete telluric correction).

### 3.3. Extinction to Individual Stars

Rough estimates for the total line-of-sight extinction (interstellar plus circumstellar) were given in §3.1.1.  $A_K$  and dereddened magnitudes can be derived for the spectroscopic targets using an adopted extinction law (Mathis 1990), the observed colors and the intrinsic colors. The latter can be estimated from the spectroscopic classifications derived in the last sections. For O stars, the intrinsic colors are small and the derived  $A_K$  depends most heavily on the extinction law and observed colors. For W43 #2 and #3, we adopt the colors for an early O star from Koornneef (1983) cited above in §3.1.1.

For WN stars, the available data are sparse. We derive intrinsic  $J - H$  and  $H - K$  using the the power law spectral indices of Morris et al. (1993). These models, derived from the observed spectral energy distributions of WR stars, characterize the emitted flux by  $F_\lambda \sim \lambda^{-\alpha}$ . For the WN7 stars analyzed by Morris et al., we find  $\alpha = 3.11 \pm 0.39$ . This corresponds to  $J - H$  and  $H - K = 0.16$  and  $0.13$ , respectively (this point is plotted in Figure 3). The uncertainty in  $\alpha$  leads to an uncertainty in each color index of  $< 0.15\ \text{mag}$ . This, in turn, leads to an uncertainty in  $A_K$  of  $< 0.25\ \text{mag}$ .

The positions of the three spectroscopic targets in Figure 3 are in good agreement with these adopted intrinsic colors. W43 #3 lies on the reddening line for an early O star, W43 #1 is close to a projected line from the colors we derive for a WN7 star, and W43 #3 is at least within the envelope for normal stars.

Using these adopted colors, we find  $A_K = 3.55\ \text{mag}$ ,  $3.52\ \text{mag}$ , and  $3.63\ \text{mag}$  for W43 #1, #2, and #3, respectively. We have averaged the derived extinction calculated using the  $J - H$  and  $H - K$  colors separately, rather than attempting to deredden along lines parallel to those in Figure 3. For typical variations in the adopted extinction law (Mathis 1990), the  $A_K$  will change by  $\lesssim 0.25\ \text{mag}$ . This uncertainty dominates over the photometric errors.

## 4. DISCUSSION

### 4.1. Similarities to Known Starburst Clusters

The dense stellar cluster at the heart of W43 with associated evolved massive stars is reminiscent of the well studied clusters in NGC 3603 (Drissen et al. 1995) in the Galaxy and R136 in the giant H II region 30 Doradus in the Large Magellanic Cloud (LMC; Massey & Hunter 1998). A common thread between these two starburst clusters and W43 is the close spatial association of apparently evolved WN stars and younger O3 stars. Our infrared spectral types are not precise enough to assign detailed sub-types for W43 #2 and W43 #3, but the latter is likely an early O star as discussed in §3.2.2. Both Drissen et al. (1995) and Massey & Hunter (1998) conclude that the WN objects are probably core hydrogen burning stars with such intense mass-loss winds that their spectra resemble the more evolved WR stars (see also de Koter et al. 1997).

The recently discovered starburst cluster 20 pc in projection from the Galactic center, the Arches cluster, is also similar to R136, NGC 3603, and W43 in that it contains many (perhaps 100) O stars (Serabyn et al. 1998) as well as WN stars (Cotera et al. 1996) in a remarkably small volume. Like W43, the Arches cluster is heavily obscured by interstellar extinction, and its stellar content can only be studied at near infrared wavelengths. Nevertheless, W43 and the Arches cluster suggest that nearby examples of the starburst phenomena are not as rare as previously thought.

### 4.2. Comments on Distance and Luminosity

In principle, the derived dereddened colors and spectral type can be used to estimate the distance to W 43. In practice, a meaningful estimate will require more spectra of stars in the cluster and additional luminosity indicators in the near infrared spectroscopic classification schemes. We plan to work on both of these aspects in the future. To illustrate the present difficulties, we consider the following.

W43 #1 has a spectral type with implicit uncertainties given the fact that, in at least one scenario (§3.2.1), it suggests a potential companion. Nevertheless, using an estimate from Vacca & Torres-Dodgen (1990) for the  $M_V$  ( $-6.54 \pm 0.43$  mag) of a typical WN7 (including those with *+abs* classifications) and a derived  $V - K$  ( $0.12 \pm 0.59$ ) from Morris et al. (1993) a lower limit to the distance can be derived:  $2800_{-900}^{+1400}$  pc. Where the uncertainty is dominated by the intrinsic scatter in  $M_V$  and systematic uncertainty in  $V - K$  due to the range of spectral index. This near distance compared to the radio distance (7 kpc;

see §1) suggests W43 #1 likely does have some contamination in the  $K$ -band brightness. Similarly, the average distance for the two O stars is:  $4300^{+1100}_{-900}$  pc using  $M_V$  ( $-6.44 \pm 0.67$  mag) from Vacca et al. 1996 and  $V - K$  ( $-0.93$ ) from Koornneef (1983). If W43 #2 and #3 are taken to be giants instead of supergiants, then the distance estimate would be  $\sim 5700$  pc.

The above discussion can be reversed and the luminosity derived instead of the distance. Adopting the radio distance of 7 kpc (see §1) and assuming all the objects are single stars, the absolute magnitudes for W43 #1, #2, and #3 are  $M_V = -8.51, -7.69, -7.28$  mag, respectively. These can be compared to the derived  $M_V$  for the most luminous O stars (Vacca et al. 1996) and WN7 stars (Vacca & Torres-Dodgen 1990):  $-6.4, -6.1$ , and  $-5.78$ , for O supergiants, giants, and dwarfs, respectively and  $-6.54$  for WN7 stars. Individual O star spectral types exhibit mean  $M_V$  as luminous as  $-7.4$  mag, and a typical standard deviation in the distribution of  $M_V$  at any spectral type is  $\sim 0.6$  mag (Vacca et al. 1996). The standard deviation in the distribution of  $M_V$  for WN7 stars (Vacca & Torres-Dodgen 1990) is 0.43 mag and the most luminous object (WR 89) has  $M_V = -7.3$  mag. At seven kpc, these numbers suggest the W43 objects (in particular, W43 #1) may be extremely luminous, as has been suggested for evolved massive stars in the center of the Galaxy (e.g., Tamblyn et al. 1996 and Figer et al. 1998). For example, W43 #1 has an estimated  $M_{\text{bol}}$  of  $-11.5$  mag compared to  $M_{\text{bol}} \leq -11.7$  mag for the Pistol star in the Galactic center Quintuplet cluster (Figer et al. 1998). The  $M_{\text{bol}}$  for W43 #1 is derived using a bolometric correction of  $-3.0$  mag (Crowther et al. 1995). Obviously, no definitive statements can yet be made for W43 with only three spectra in hand and in the face of the substantial uncertainties outlined here.

Intrinsic colors and magnitudes for rare spectral types like W43 #1 may always provide difficulties. However, the colors for more normal O and B stars are well understood. As our spectral classification schemes improve and we obtain spectra of fainter O and B stars in the cluster, we will be able to better assess the distance to W43 and the luminosity of the individual stars. It is already clear that clusters like W43 will be very important in comparison to the Galactic center star clusters and to the further study of massive stars in the Milky Way.

### 4.3. Star Formation

The combination of the Lester et al. (1985) far infrared maps and the present near infrared images and spectra suggest the following scenario. The stellar cluster appears between the strongest far infrared sources (G30.08 N and S) in a region of lower dust

emission. The evolved nature of the central massive stars in the cluster and lower dust emission indicate the central cluster may have formed first and subsequently cleared away the remains of the gas and dust which came together to form it (or is in the process of clearing it away: there are dark regions very close in projection to the central cluster). The embedded red objects seen in Figure 4 in the regions coincident with the far infrared sources G30.08 N and S may be newly forming stars more deeply embedded in the molecular clouds now being ionized by the central cluster (and to some extent by massive stars forming within). We will test this scenario by searching for spectroscopic signatures of YSOs in the brighter embedded objects in G30.08 N and S.

## 5. SUMMARY

Near infrared images reveal a dense cluster of newly formed stars at the core of the Galactic giant H II region W43. Spectra of three of the brightest cluster members show them to be hot, massive stars. The brightest member, W43 #1, has a  $K$ -band spectrum very similar (in morphology as well as line strength and width) to similar spectra for optically classified WR stars of the WN7 type. Recent observations near the Galactic center, in NGC 3603, and in R136 in the LMC all find WN type stars at the center of dense starburst clusters. A picture is emerging where these objects are thought to be core burning H stars with extreme mass-loss, rather than the somewhat older evolved counterparts of initially massive O stars.

The combination of  $J$ ,  $H$ , and  $K$  images reveals a complex morphology in the region surrounding the stellar cluster. In particular, the spatial geometry suggests the starburst cluster may have triggered second generations of stars to form in the molecular material to the North and South. Both these regions are locations of far infrared emission maxima which suggest even younger stars still more highly obscured.

It is a pleasure to acknowledge the help of J. Holtzman in installing the latest version of LickVista (5.0) on RDB's new Linux box. We appreciate the availability and support of quality tools like LickVista. We also thank R. Pogge for his Liner program used to analyze spectra presented here. We kindly acknowledge suggestions from an anonymous referee which have improved our paper. PSC appreciates support by the NSF under grant 97-31520. A.D. thanks PRONEX/FINEP for financial support. Support for this work was provided by NASA through grant number HF 01067.01 – 94A from the Space Telescope Science Institute, which is operated by the Association of Universities for Research in Astronomy, Inc., under NASA contract NAS5-26555.

## REFERENCES

- Blum, R.D., Ramond, T.M., Conti, P.S., Figer, D.F, & Sellgren, K. 1997, AJ, 113, 1855
- Conti, P. S., Hanson, M. M., Morris, P. W., Willis, A. J., & Fossey, S. J. 1995, ApJ, 445, L35
- Cotera, A., Erickson, E. F., Colgan, S. W. J., Simpson, J. P., Allen, D. A., & Burton M. 1996, ApJ, 461, 750
- Cotera, A. & Simpson J. 1997, AAS meeting 191, abstract 114.03
- Crowther, P. A., Hillier, D. J., & Smith L. J. 1995 A&A, 293, 403
- DePoy, D. L., Gregory, B., Elias, J., Montane, A., Pérez, G., & Smith, R. 1990, PASP, 102, 1433
- de Koter, A., Heap, S. R., & Hubeny, I. 1997, ApJ477, 792
- Drissen, L., Moffat, A. F. J., Walborn, N. R., & Shara, M. M. 1995, AJ, 110, 2235
- Eenens, P. R. J., Williams, P. M., & Wade, R. 1991, MNRAS, 252, 300
- Figer, D. F., McLean, I. S., & Najarro, F. 1997, ApJ, 486, 420
- Figer, D. F., Najarro, F., Morris, M., McLean, I. S., Geballe, T. R., Ghez, A. M., & Langer, N. 1998, ApJ, 506, 384
- Frogel, J. A., Persson, S. E., Aaronson, M., & Matthews, K. 1978, ApJ, 220, 75
- Hanson, M. M., Conti, P. S., & Rieke, M. J. 1996, ApJS, 107 281 (HCR96)
- Hanson, M.M., Howarth, I.D., & Conti, P.S. 1997, ApJ, 489, 698
- Koornneef, J. 1983, A&A, 128, 84
- Lester, D.F., Dinerstein, H.L., Werner, M.W., Harvey, P.M., Evans II, N.J., & Brown, R.L. 1985, ApJ, 296, 565
- Liszt, H.S., Braun, R., & Greisen, E.W. 1993, AJ, 106, 2349
- Liszt, H.S. 1995, AJ, 109, 1204
- Massey, P., Johnson, K., & DeGioia-Eastwood, K. 1995, ApJ, 454, 151
- Massey, P. & Hunter, D. A. 1998, ApJ, 493, 180
- Mathis, J.S. 1990, ARA&A, 28, 37
- Morris, M. & Serabyn, E. 1996, ARA&A, 34, 645
- Morris, P. W., Brownsberger, K. R., Conti, P. S., Massey, P., & Vacca, W. D. 1993, ApJ, 412, 324

- Olivia, E. & Origlia, L. 1992, A&A, 254, 466
- Pérez, G. & Elston, R. 1998, to appear in SPIE proceedings on Instrumentation in Astronomy
- Persson, S. E., Murphy, D. C., Krzeminski, W., & Roth, M. 1998, AJ, in press
- Probst, R., Ellis, T., Fowler, I., Gatley, I., Heim, G., & Merrill, K. 1994, SPIE proceedings on Instrumentation in Astronomy VIII, 2198, 695
- Schmidt–Kaler, T. 1982, in Landolt–Börstein, New Series, group VI, vol. 2, ed. K. Schaifers & H. H. Voigt (Berlin: Springer–Verlag), 1
- Smith, L.F., Biermann, P. & Mezger, P.G. 1978, A&A, 66, 65
- Stetson, P. 1987, PASP, 99, 191
- Subrahmanyan, R. & Goss, W.M., MNRAS281, 239
- Tamblyn, P., Rieke, G. H., Hanson, M. M., Close, L. M., McCarthy, D. W., JR., & Rieke, M. J. 1996, ApJ, 456, 206
- Vacca, W. D. 1994, ApJ, 421, 140
- Vacca, W. D. & Torres–Dogden A. V. 1990, ApJS, 73, 685
- Vacca, W. D., Garmany, C. D., & Shull, J. M. 1996, ApJ, 460, 914

Table 1. W43 #1  $K$ -band Spectra Data

Line Id ( $\mu\text{m}$ )	FWHM ( $\text{\AA}$ )	EW ( $\text{\AA}$ )
2.0378 He II	144	5
2.1127 He I, 2.1155 N III	103	11
2.1661 H I	160	48
2.1892 He II	109	11

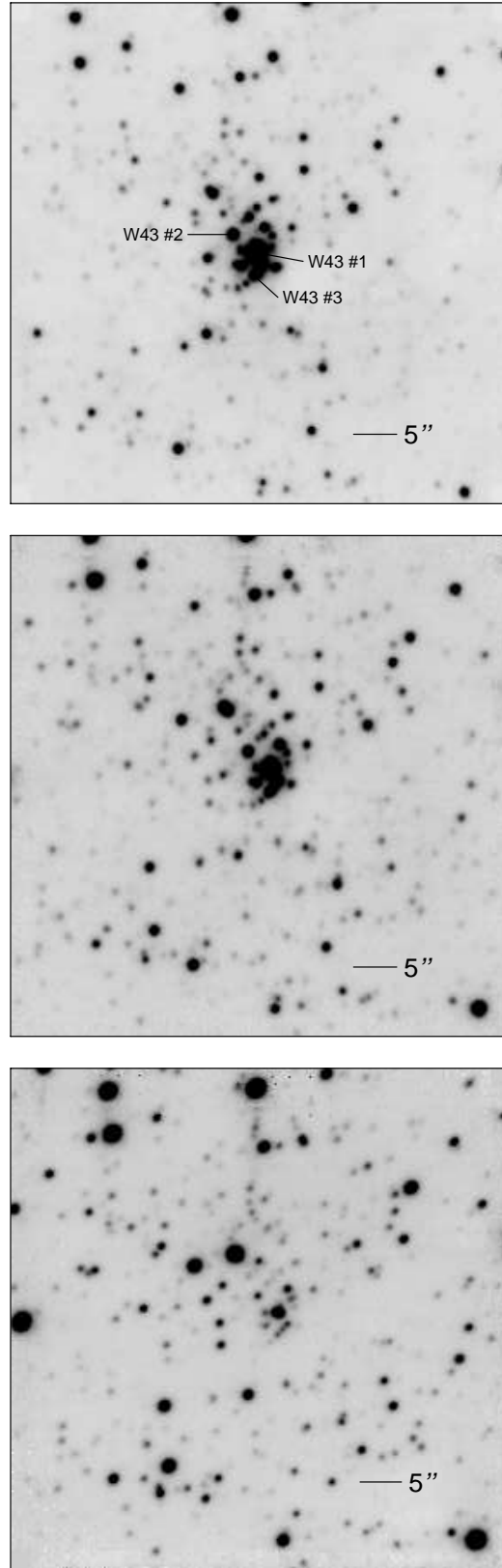


Fig. 1.— High resolution CIRIM images of the W43 central cluster.  $K$  (2.2  $\mu\text{m}$ ) is at the top,  $H$  (1.65  $\mu\text{m}$ ) in the middle, and  $J$  (1.25  $\mu\text{m}$ ) at the bottom. North is up, East to the left. Three of the brightest four stars in the central  $\sim 5''$  have spectra presented in Figures 5, 6, and 7.



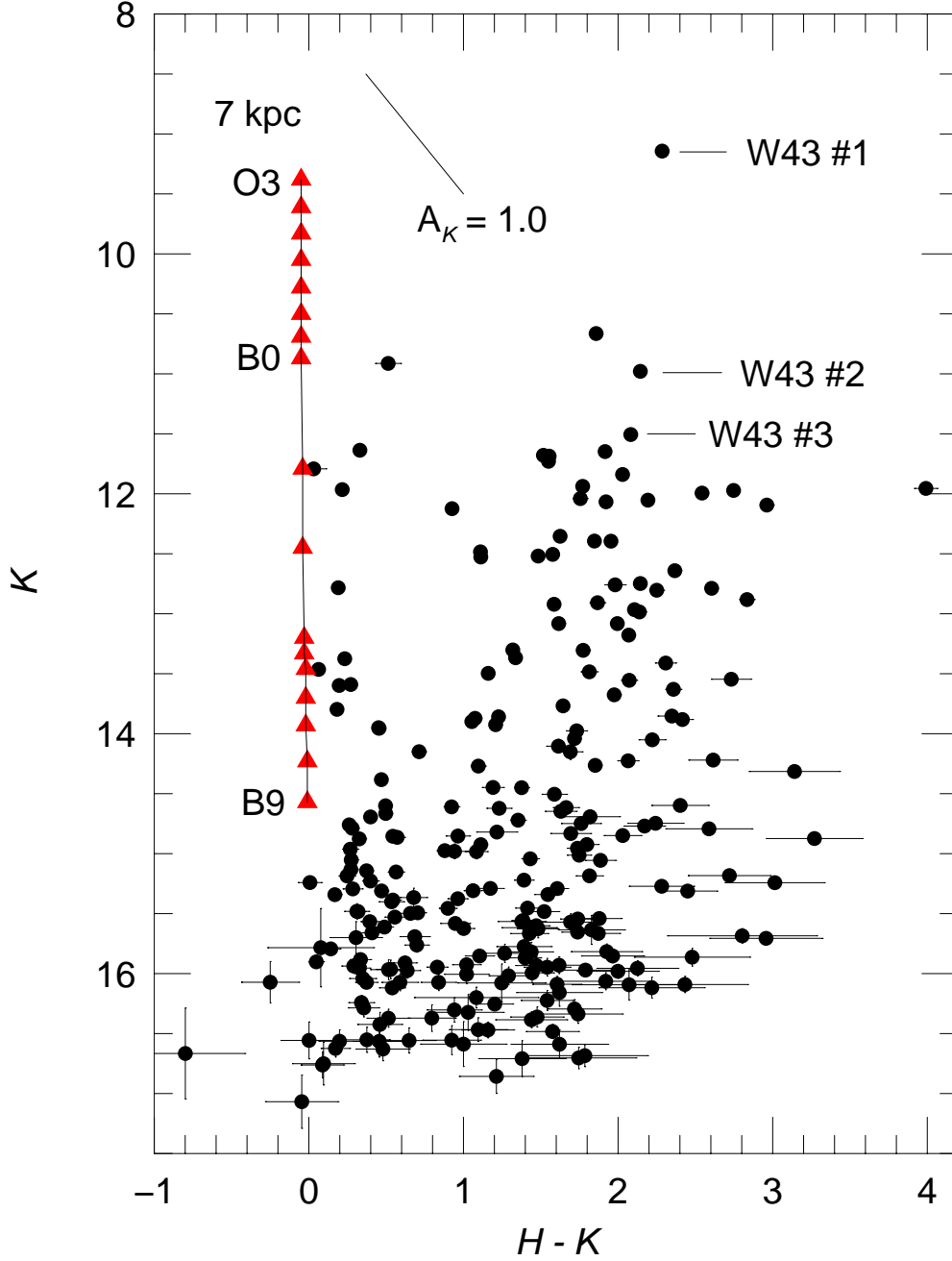


Fig. 2.—  $H - K$  color-magnitude diagram (CMD) for the W43 cluster. Data are from the high angular resolution CIRIM images. A foreground sequence is clearly present as well as a cluster sequence and a number of very red stars. Stars for which spectra are presented are labeled. The main sequence is plotted as *filled* triangles for spectral types O3 to B9 at a distance of 7 kpc.

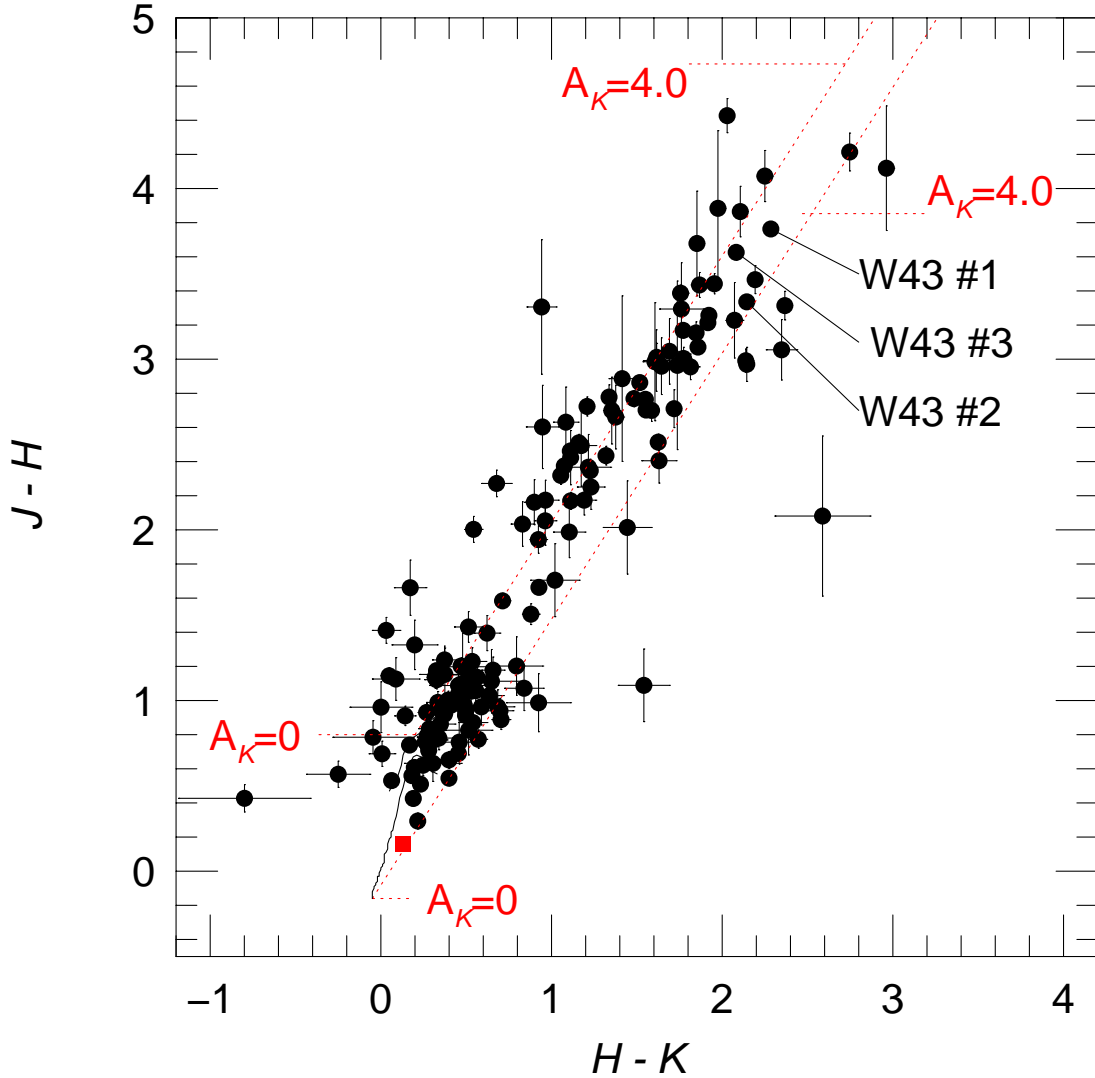


Fig. 3.—  $J-H$  vs.  $H-K$  color-color diagram for the region around the W43 cluster. W43 #1, #2, and #3, for which spectra are presented, are labeled. No strong color excess is indicated for W43 #1, #2, or #3 by comparison with the reddening lines for early O stars ( $H-K = -0.05$ ,  $J-H = -0.16$ ) or M giants ( $H-K = 0.2$ ,  $J-H = 0.8$ ). The color-color relation for un-reddened main sequence stars (Koornneef 1983) and late-type giants (Frogel et al. 1978) is also shown for comparison. The *square* point is the derived color for a WN7 star; see text.

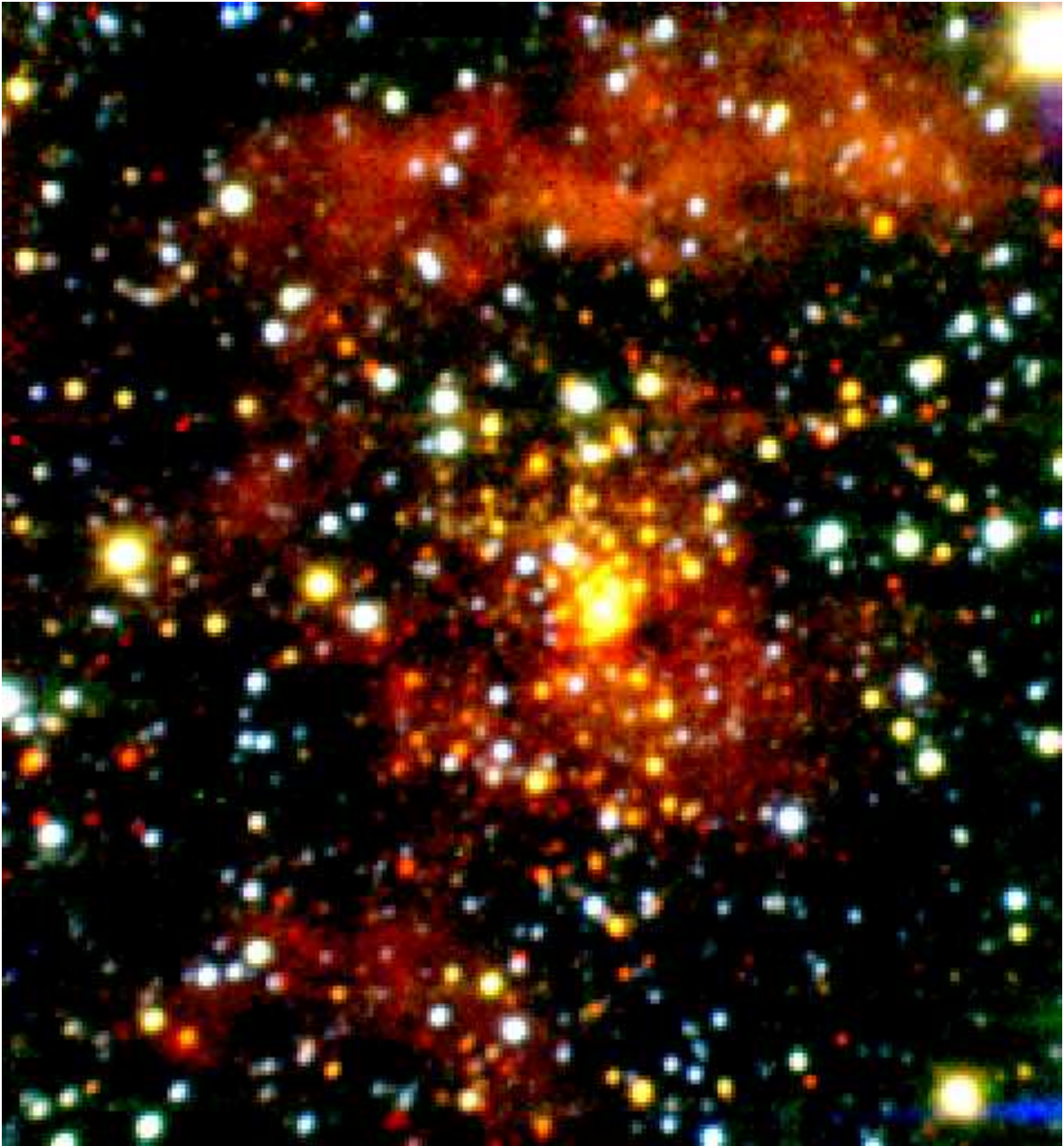


Fig. 4.— *JHK* color composite image of the W43 cluster and surrounding field made from the  $0.65'' \text{ pix}^{-1}$  CIRIM images (*J* is coded blue, *H* green, and *K* red). North is up, East to the left. The field of view is approximately  $2.7' \times 2.7'$ . There is strong differential reddening in the field (see text) with darker clumps of material quite close in projection to the central cluster (e.g.  $\sim 5''$  SW). The E–W nebulosity at the top is the region G30.8N in the terminology of Lester et al. (1985); the nebulosity to the SE of the cluster is G30.8S.

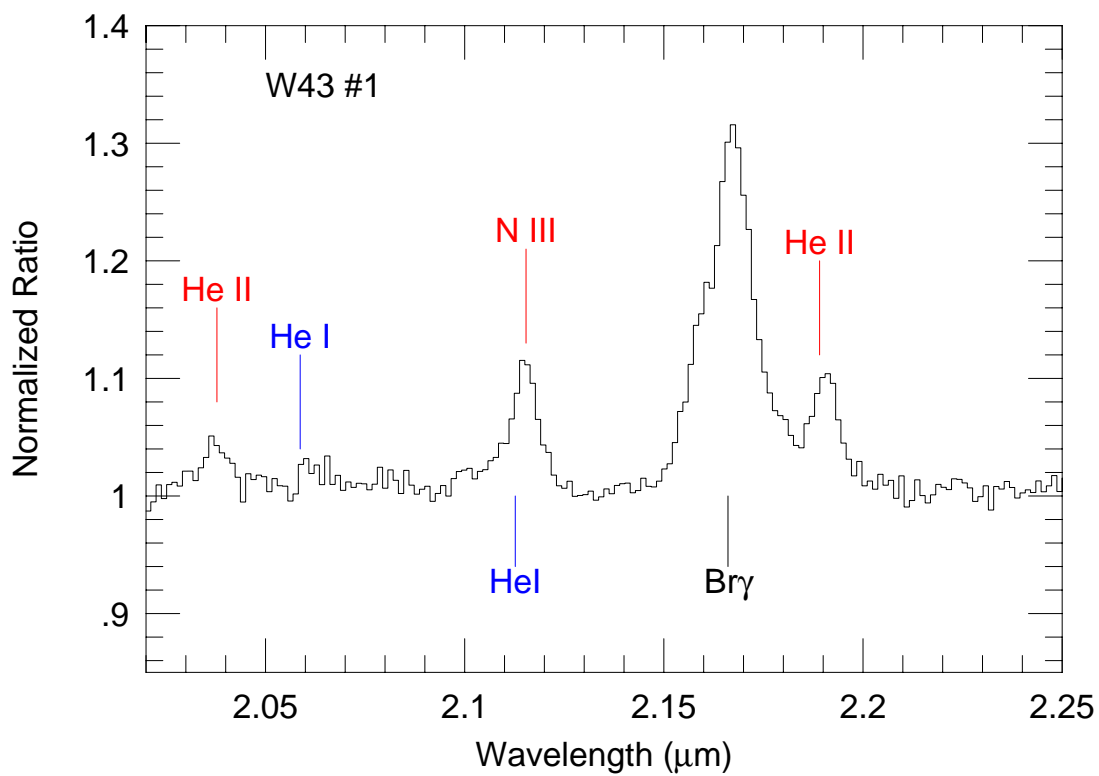


Fig. 5.— W43 #1, the brightest star of the W43 cluster. Comparison to similar spectra of known Wolf-Rayet (WR) stars in Figer et al. (1997) indicates this object is a member of the nitrogen sequence (WN7).

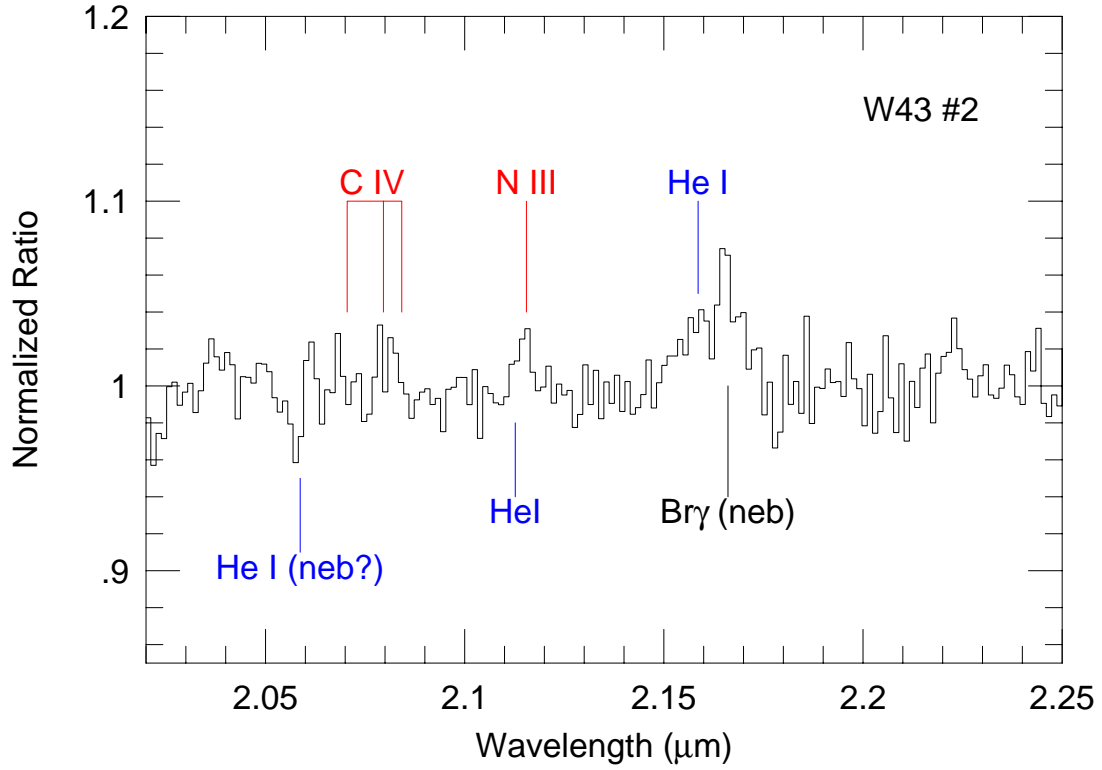


Fig. 6.— W43 #2. Comparison to similar spectra of known hot stars from Hanson et al. (1996) suggests this is an early O type supergiant. The  $\text{Br}\gamma$  emission is probably nebular in origin; its contribution is highly non-uniform along the slit. Similarly, the He I  $2.06\ \mu\text{m}$  line is possibly over-subtracted nebular emission. Positions of other He I lines are indicated, though the lines are not necessarily detected.

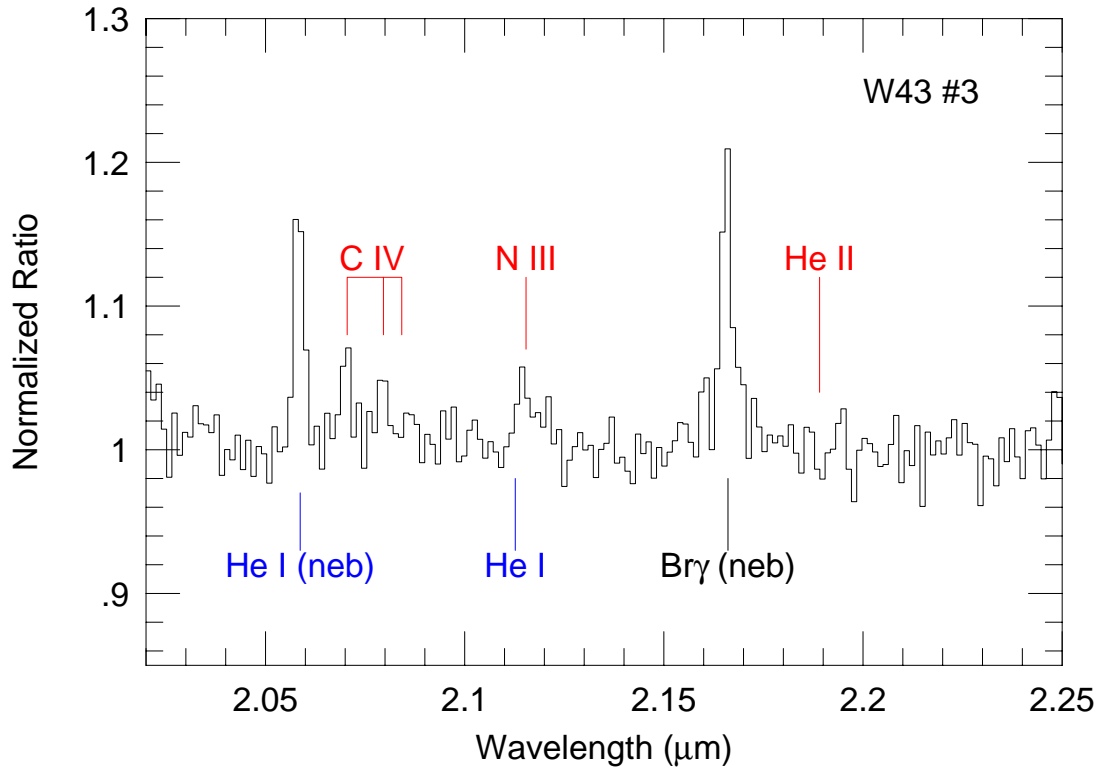


Fig. 7.— W43 #3. Comparison to similar spectra of known hot stars from Hanson et al. (1996) suggests this is an early O type supergiant. The  $\text{Br}\gamma$  and He I  $2.06\ \mu\text{m}$  features are probably nebular; see text.